

## Localization in Artificial Disorder: Two Coupled Quantum Dots

M. Brodsky,\* N. B. Zhitenev,<sup>†</sup> and R. C. Ashoori

*Department of Physics, Massachusetts Institute of Technology, Cambridge, Massachusetts 02139*

L. N. Pfeiffer and K. W. West

*Bell Laboratories, Lucent Technologies, Murray Hill, New Jersey 07974*

(Received 14 January 2000)

Using single electron capacitance spectroscopy, we study electron additions in quantum dots containing two potential minima separated by a shallow barrier. Analysis of the addition spectra in the magnetic field allows us to distinguish between electrons delocalized over the entire dot and those localized in either of the potential minima. We demonstrate that a high magnetic field abruptly splits up a low-density droplet into two smaller fragments, each residing in a potential minimum. An unexplained cancellation of electron repulsion between electrons in these fragments gives rise to paired electron additions.

PACS numbers: 73.20.Dx, 73.20.Jc, 73.23.Hk

For half a century physicists have worked to understand localization of strongly interacting electrons in a disordered potential. Either electron interactions or disorder can produce localization [1,2]. Though their interplay in two-dimensional systems has been a subject of intense experimental and theoretical studies [3,4], no theory exists fully describing the effects of both disorder and strong interaction.

Quantum dots provide a convenient system for studying electron localization on a microscopic scale. However, the traditional transport techniques for studying lateral quantum dots [5] sense primarily delocalized electronic states. A possible exception is transport studies in vertical structures, but these do not permit variation of electron density [6], a critically important parameter that changes the effective strength of electron interactions. We study electron additions in vertical quantum dots using single electron capacitance spectroscopy (SECS) [7]. It has demonstrated the capability of probing both *localized* and delocalized states of electrons. Furthermore, this method allows us to study 2D dots of various sizes and over a broad range of electron densities.

In quantum dot experiments in high-density dots, the Coulomb repulsion between electrons largely sets the amount of energy required to add an additional electron to the dot. This energy increases by a fixed amount with each electron added. An external gate, capacitively coupled to the dot, can then be used to change the electron number, and electron additions occur periodically in the gate voltage with a period  $e/C_g$ , where  $C_g$  is the capacitance between the gate and the dot [5].

In contrast, our prior SECS measurements have shown that the *low-density* regime appears entirely different. The addition spectrum of a 2D-electron droplet larger than  $0.2 \mu\text{m}$  in diameter and below a critical electron density ( $n_0 = 1 \times 10^{11} \text{ cm}^{-2}$  in all of our samples) is highly non-periodic. It contains pairs and bunches: two or more successive electrons can enter the dot with nearly the same energy [7,8]. The paired electrons thus show almost no

sign of repelling each other. Application of high perpendicular magnetic field increases  $n_0$  linearly, creating a sharp *boundary* between periodic and “paired” parts of the addition spectrum [8]. We hypothesized that, for densities below this boundary, disorder and electron-electron interactions within the low-density droplet split it into two or more spatially separate droplets, and pairing arises once this localization occurs. We have produced experiments to study this localization-delocalization transition in a controlled fashion. One recently established the existence of electronic states localized at the dot’s periphery and arising at densities just below the critical density  $n_0$  [9].

In this Letter we report the results of a new approach for studying localization and pairing in quantum dots. We intentionally create a dot with an artificial “disorder” potential: a potential profile containing two smooth minima separated by a barrier, as in the double dot system described below. Through analysis of addition spectra in magnetic field, we distinguish between electrons either localized in potential well or delocalized over the entire dot. Our studies conclusively demonstrate that under precisely the same conditions for observation of the paired electron additions a low-density electron droplet inside the dot indeed splits up into smaller fragments. This abrupt disintegration creates a sharp *boundary* between periodic and paired parts of the addition spectra, with paired electrons entering into spatially distinct regions within a dot. We also measure the remnant residual interaction between the fragments. Surprisingly, it displays a nearly complete independence on the strength of the applied field for fields larger than required for the localization transition. While no theory exists explaining the observed transition or the pairing phenomenon, recent numerical simulations display results similar to some of our data [10].

The dots were fabricated within an AlGaAs/GaAs heterostructure as described in previous work [7,8]. The essential layers (from bottom to top) are a conducting layer of GaAs serving as the only contact to the dots, a shallow AlGaAs tunnel barrier, a GaAs active layer that contains

the dots, and an AlGaAs blocking layer. On the top surface, we produce a small AuCr top gate using electron beam lithography. This top gate was used as a mask for reactive ion etching that completely depletes the active GaAs layer in the regions away from the AuCr gate.

To create a barrier within a dot we pattern a top gate in a dumbbell shape. This produces two small vertical dots laterally separated by a small distance (a schematic of our samples is shown in Fig. 1b). The top gate controls the electron density of the entire system. This geometry results in a double potential well with two valleys separated by a saddle. By changing the top gate bias  $V_g$ , we gradually fill the double dot system with electrons. At first electrons accumulate in two independent electron puddles, one localized in each dot. The puddles grow laterally with increasing electron number and eventually couple to each other. The coupling mixes states of one dot with those of the other, and electrons start traversing the saddle point. When the two puddles finally merge into a single large dot, the electron wave functions spread over the entire area of the resulting large dot.

By varying lithographic dimensions, we control the height of the saddle and therefore the individual dot electron density at which merging occurs. We examine a number of samples to investigate a broad range of such densities: from two dots each containing a few localized electrons up to densities  $n = (2.5-3.5) \times 10^{11} \text{ cm}^{-2}$  in each dot.

The measurements are carried out using the on-chip bridge circuit described in [7]. To register electron additions, we monitor the ac capacitive response to a small ( $<80 \mu\text{V}$ ) ac excitation applied between the top gate and the contact layer. Since one top gate covers both individual dots, an electron addition to either of the dots results in a peak [7] in our capacitance measurements.

To distinguish electrons added to one dot from those added to the other, we follow the evolution of the addition spectrum with perpendicular magnetic field. The general behavior of the electron addition spectrum for a single dot in magnetic field is well known both for the case of few-electron droplets [6,11] and for many-electron dots in quantum Hall regime [12,13]. Addition energies oscillate with field as electrons shift between different angular momentum states. The exact pattern of those oscillations depends sensitively on the details of the confinement potential, and serves as a "signature" of a particular dot. Although in our samples the two dots are made to be nominally identical, the particular shapes of the confinement potential of the two dots are slightly different due to disorder and imperfections in the lithography process. Addition energies for the two dots thus depend differently on the perpendicularly applied magnetic field, permitting us to associate each electron addition with a particular dot.

The capacitance traces taken at different values of the magnetic field are plotted together on the grey scale panel in Fig. 1a. Black denotes high capacitance. Each successive trace corresponds to the energy for adding an

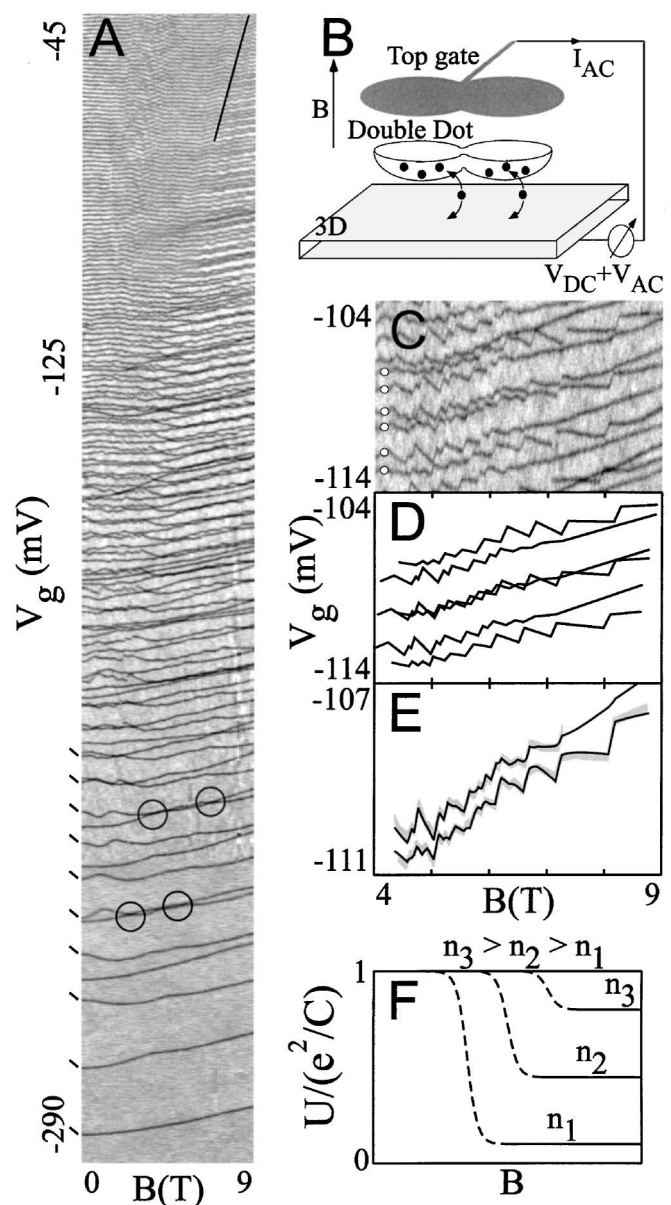


FIG. 1. (b) Schematic of our samples. The dot potential profile contains two minima separated by a barrier. A single top gate controls the electron densities of the entire two-dot system. (a) Grey scale plot of quantum dot capacitance as a function of gate bias and magnetic field. Black denotes high capacitance. Each successive trace corresponds to the energy for adding an electron to the double dot system. First 10 additions to one dot are marked by dashes. Circles mark level crossings. A diagonal line delineates a clearly visible sharp *boundary* described in the text. (c) An addition spectrum expanded to the right of the boundary. Six subsequent addition traces marked by empty circles are  $R_1, B_1, H_1, H_2, B_3, R_3$  (bottom to top).  $R_1, R_3$  and  $B_1, B_3$  represent two oscillation patterns. Hybridized traces  $H_1, H_2$  do not belong to any of the patterns. (d) The hypothetical spectrum in absence of the interaction between two dots. Hybrid states  $H_1, H_2$  are replaced by two unperturbed independent states from two dots:  $R_2, B_2$ . (e) Reconstruction of the hybrid states. The data ( $H_1, H_2$ ) are shown in grey; black are fits. (f) Schematic field dependence of the tunneling matrix element  $U$  for different densities ( $n_1 < n_2 < n_3$ ). Solid lines denote regions where residual coupling is extracted, as described in the text.

electron to the double dot system. The lowest trace shown represents the first electron added to the two-dot system. The low-density part of the spectrum ( $-290 \text{ mV} < V_g < -135 \text{ mV}$ ) appears as a simple superposition of two different families of traces. The first ten electron addition traces comprising one family are marked by dashes. Each family can be described qualitatively within the constant interaction model for Darwin-Fock states, as is typical for individual small circular dots [6,11,14]. Because such separation of the spectrum is possible, we conclude that up to  $V_g = -135 \text{ mV}$  our system consists of two independent electron droplets. Incidental alignment of the ground states of the two droplets for some particular values of the gate bias and the magnetic field may cause simultaneous but independent electron additions to each individual dot. Indeed, multiple level crossings (some marked by circles in Fig. 1a) can be seen on the plot. At each crossing point the peak in the capacitance signal has double height, indicating an independent addition of two electrons to the two-dot system. The exact coincidence of the peaks suggests that capacitive coupling between two droplets is negligible. At much higher densities ( $V_g > -45 \text{ mV}$ ) there is only one periodic Coulomb ladder, indicating that the initially separate electron droplets have merged into a single one.

The transition between the two limits occurs over gate biases  $-135 \text{ mV} < V_g < -45 \text{ mV}$ , depending on the strength of the applied magnetic field. At zero field, the merging occurs in an interval  $\Delta V_g = 25 \text{ mV}$  wide centered around  $V_g = -125 \text{ mV}$ . The gate bias  $V_g = -125 \text{ mV}$  corresponds to electron densities in each individual dot of  $1.2 \times 10^{11} \text{ cm}^{-2}$  and  $1.7 \times 10^{11} \text{ cm}^{-2}$ , respectively. Each dot contains about 30 electrons. For higher densities and at zero field there is one combined dot under the gate. However, magnetic field greater than 4 T dramatically affects the spectrum. There exists a clearly visible sharp boundary, which separates the spectrum into two parts. It is marked by a line in Fig. 1a. To the left of the boundary (the low field side), all electron addition traces show similar evolution with magnetic field; electrons appear to enter one combined dot and Coulomb blockade produces nearly periodic addition spectrum. To the right of the boundary (the high field side), the periodicity of the spectrum is broken, and many anomalous, closely spaced electron additions are seen. With increasing magnetic field, the boundary between the two regimes extends up to densities of  $1.7 \times 10^{11} \text{ cm}^{-2}$  and  $2.2 \times 10^{11} \text{ cm}^{-2}$ , in each dot, respectively (over 60 total electron additions to the two-dot system). An increase in density of each dot along the boundary can be approximated by the linear relation  $\Delta n \propto 0.1 \times B(T) \times 10^{11} \text{ cm}^{-2}$  for both of the two individual dots. This linear relation holds for all of our samples. Surprisingly, this boundary follows the same linear density-field relation as the one seen in individual dots of larger sizes [8].

To understand the origin of this boundary we expand the addition spectrum to the right of the boundary (Fig. 1c) and focus on six marked subsequent addition traces  $R1, B1,$

$H1, H2, B3, R3$ . All of the marked traces again oscillate with magnetic field. But here the origin of the oscillations is different from that of the few-electron case considered above. For magnetic field higher than 4 T, electrons within each dot fill only the lowest orbital Landau level, but with both spin-up and spin-down electrons. With increasing magnetic field, the electron orbits shrink and Coulomb repulsion causes redistribution of electrons between the two spin-split branches of the lowest orbital Landau level. This produces oscillations in the single electron traces known as “spin flips” [5,12,13].

Figure 1c shows two different oscillation patterns. One is represented by traces  $R1$  and  $R3$ ; similarly, traces  $B1$  and  $B3$  display another pattern. In fact, the entire spectrum can be separated into two nearly periodic Coulomb blockade sets, which differ by their “spin flip” patterns. Since addition traces within each set are widely separated by Coulomb blockade, any two traces that appear close to each other belong to *different* sets. The existence of two patterns characteristic of the individual dots indicates that to the right of the boundary there exist two separate dots, despite the fact that for zero field two dots are merged into one. We conclude that the boundary separates two regimes in  $V_g - B$  space. In one regime, electron wave functions are spread over the entire area of the double dot, and in the other each electron dwells in one of two individual dots.

In the latter regime, the two dots are not completely independent. Though magnetic field breaks one combined electron dot into two separate ones, residual coupling remains. The barrier between the two dots is small, and inter-dot tunneling remains possible [15]. When ground states of individual dots are aligned with each other, a finite tunnel coupling splits two aligned levels [16,17]. Such alignment creates the equivalent of a molecular hybrid state. Examples of such splitting are the two hybridized traces in the middle of the plot in Fig. 1c:  $H1, H2$ . They cannot be solely associated with either of the two spin flip patterns but rather exhibit features belonging to both of them. The hybridization shown is not a rare occurrence. Each pair of closely spaced traces mixes into a hybrid.

We estimate the coupling strength between two dots by describing the spectra using single particle states. We reconstruct the two hybridized states  $H1$  and  $H2$  from the neighboring “one-dot states”  $R1, B1, B3, R3$  in the following way. First, we assume that in the absence of a residual interaction the spectrum would be as presented in Fig. 1d. In place of the hybrid states  $H1, H2$  there are two unperturbed independent states from the two dots:  $R2$  and  $B2$ . For these unperturbed states we take  $E_2^R = (E_1^R + E_3^R)/2$  and  $E_2^B = (E_1^B + E_3^B)/2$ . Second, we assume that tunneling between  $R2$  and  $B2$  produces an off-diagonal matrix element  $U$ . Diagonalization of the Hamiltonian

$$\begin{bmatrix} E_2^B & U \\ U^* & E_2^R \end{bmatrix}$$

splits  $E_2^R$  and  $E_2^B$  into a pair of hybrid states,

$$E_{1,2}^H = \frac{(E_2^R + E_2^B)}{2} \pm \sqrt{\frac{(E_2^R - E_2^B)^2}{4} + U^2}. \quad (1)$$

Surprisingly, for such a simplistic model using  $U$  as the only fitting parameter, we obtain practically perfect fits to our data (Fig. 1e). Unexpectedly, the residual coupling strength  $U$  [ $U \approx 0.1 \times (e^2/C_{\text{dot}})$  for the case shown] displays nearly complete independence of the strength of the applied field for fields larger than required for the localization transition.

The results of similar fitting for different densities are summarized in Fig. 1f. Though constant in field, this coupling increases with density, and becomes comparable to  $E_c = e^2/C_{\text{dot}}$  at densities around  $2 \times 10^{11} \text{ cm}^{-2}$ . The boundary ceases to exist at these densities. In fact, the boundary is altogether absent in samples for which the individual dot densities at the merging point are higher than  $2.3 \times 10^{11} \text{ cm}^{-2}$ ; i.e., magnetic field has no effect on the merging of two high-density dots.

Our data convincingly establish that high magnetic field abruptly splits a low-density electron droplet placed in disorder potential into smaller fragments. It is this split up that causes a sharp boundary in the addition spectrum. The paired electron additions to the dot seen to the right of the boundary result from an unexplained cancellation of electron repulsion between electrons in these fragments. The boundary essentially separates two phases: in one, electrons are delocalized over the entire sample, and, in the other, electrons are confined in local disorder minima. We believe that a similar scenario takes place in large single dots, in which real disorder is present [8]. In that case the boundary is presumably related to a breakup of the larger droplet into a central core and localized periphery.

The physical mechanism of such separation or of the pairing phenomena has yet to be established. However, a recent preprint [18] shows that a two-phase coexistence of a high-density liquid and a low-density gas might be energetically favorable in the interacting two-dimensional system placed in disorder potential, and numerical calculations by Canali [10] support our finding that two electrons in the pair enter into spatially separated regions of the dot.

We acknowledge useful discussions with C. de C. Chamon, H. B. Chan, G. Finkelstein, D. Goldhaber-Gordon, B. I. Halperin, M. A. Kastner, L. S. Levitov, and K. A. Matveev. Expert etching of samples was performed by S. J. Pearton. This work is supported by the ONR, JSEP-DAAH04-95-1-0038, the Packard Foundation, NSF DMR-9357226, and DMR-9311825.

\*Email address: misha@electron.mit.edu

†Present address: Bell Laboratories, Lucent Technologies, Murray Hill, NJ 07974.

- [1] N. F. Mott, Proc. Phys. Soc. London, Ser. A **62**, 416 (1949).
- [2] P. W. Anderson, Phys. Rev. **109**, 1472 (1958).
- [3] S. V. Kravchenko, G. V. Kravchenko, J. E. Furneaux, V. M. Pudalov, and M. D'Iorio, Phys. Rev. B **50**, 8039 (1994); D. Popovic, A. B. Fowler, and S. Washburn, Phys. Rev. Lett. **79**, 1543 (1997).
- [4] D. Belitz and T. R. Kirkpatrick, Rev. Mod. Phys. **66**, 261 (1994); B. L. Altshuler and A. G. Aronov, in *Electron-Electron Interaction in Disordered Systems*, edited by M. Pollak and A. L. Efros (North-Holland, Amsterdam, 1985); P. A. Lee and T. B. Ramakrishnan, Rev. Mod. Phys. **57**, 287 (1985).
- [5] M. A. Kastner, Phys. Today **46**, No. 4, 24 (1993).
- [6] S. Tarucha, D. G. Austing, T. Honda, R. J. van der Hage, and L. P. Kouwenhoven, Phys. Rev. Lett. **77**, 3613 (1996).
- [7] R. C. Ashoori, H. L. Stormer, J. S. Weiner, L. N. Pfeiffer, S. J. Pearton, K. W. Baldwin, and K. W. West, Phys. Rev. Lett. **68**, 3088 (1992); R. C. Ashoori *et al.*, Physica (Amsterdam) **189B**, 117 (1993).
- [8] N. B. Zhitenev, R. C. Ashoori, L. N. Pfeiffer, and K. W. West, Phys. Rev. Lett. **79**, 2308 (1997); R. C. Ashoori *et al.*, Physica (Amsterdam) **3E**, 15 (1998).
- [9] N. B. Zhitenev, M. Brodsky, R. C. Ashoori, L. N. Pfeiffer, and K. W. West, Science **285**, 715 (1999).
- [10] C. M. Canali, Phys. Rev. Lett. **84**, 3934 (2000).
- [11] R. C. Ashoori, H. L. Stormer, J. S. Weiner, L. N. Pfeiffer, K. W. Baldwin, and K. W. West, Phys. Rev. Lett. **71**, 613 (1993); R. C. Ashoori, Nature (London) **379**, 413 (1996).
- [12] P. L. McEuen, E. B. Foxman, J. Kinaret, U. Meirav, M. A. Kastner, N. S. Wingreen, and S. J. Wind, Phys. Rev. B **45**, 11 419 (1992).
- [13] O. Klein, C. de C. Chamon, D. Tang, D. M. Abusch-Magder, U. Meirav, X.-G. Wen, M. A. Kastner, and S. J. Wind, Phys. Rev. Lett. **74**, 785 (1995).
- [14] For a review see L. P. Kouwenhoven, C. M. Marcus, P. L. McEuen, S. Tarucha, R. M. Westervelt, and N. S. Wingreen, in *Mesoscopic Electron Transport*, edited by L. L. Sohn, L. P. Kouwenhoven, and G. Schön, NATO ASI, Ser. E (Kluwer Academic Publishers, Dordrecht, 1997), and references therein.
- [15] C. Livermore, C. H. Crouch, R. M. Westervelt, K. L. Campman, and A. C. Gossard, Science **274**, 1332 (1996), and references therein.
- [16] K. A. Matveev, L. I. Glazman, and H. U. Baranger, Phys. Rev. B **53**, 1034 (1996); **54**, 5637 (1996).
- [17] J. M. Golden and B. I. Halperin, Phys. Rev. B **53**, 3893 (1996); **54**, 16 757 (1996).
- [18] Junren Shi, Song He, and X. C. Xie, Phys. Rev. B **60**, R13 950 (1999).